



Echocardiographic strain imaging: what do paediatric cardiologists need to know?

Yiu-Fai Cheung

Division of Paediatric Cardiology, Department of Paediatrics and Adolescent Medicine, Queen Mary Hospital, The University of Hong Kong, Hong Kong, China

Correspondence to: Prof. Yiu-Fai Cheung, Department of Paediatrics and Adolescent Medicine, The University of Hong Kong, Queen Mary Hospital, 102, Pokfulam Road, Hong Kong, China. Email: xfcheung@hku.hk.

Abstract: Assessment of systolic and diastolic function of both the left and right ventricles is an integral part of the assessment and management of children with heart disease. Despite corrective or palliative repair of congenital heart disease, dysfunction of the systemic ventricle, which may be a morphologic left or a right ventricle, subpulmonary right ventricle, and the functional single ventricle may occur in the long term. Conventional echocardiographic indices of cardiac function can be regarded as parameters of indirect changes consequential to the shortening and lengthening of the myocardium in the cardiac cycle. Direct interrogation of myocardial deformation, on the other hand, may shed important lights on the understanding, diagnosis and prognosis of cardiac dysfunction in the paediatric cardiac population. In the past decade, technological advances in echocardiographic strain imaging have enabled direct interrogation of global and regional deformation of the myocardium. In this review, the concept of strain imaging, the evolution of echocardiographic strain imaging, the methods of ventricular and atrial strain quantification, and clinical applications of strain imaging in children and young adults with congenital heart disease are discussed. The gaps and challenges in the clinical translational use of echocardiographic strain imaging are also highlighted. Given the emerging data on potential prognostic values of strain measures in the prediction of occurrence of adverse cardiovascular outcomes in the congenital heart population, it is timely for paediatric cardiologists to consider the incorporation of strain imaging into the clinical management algorithm.

Keywords: Strain imaging; echocardiography; paediatrics; congenital heart disease

Received: 20 April 2021; Accepted: 18 September 2021; Published: 28 November 2022.

doi: 10.21037/pm-21-39

View this article at: <https://dx.doi.org/10.21037/pm-21-39>

Introduction

Assessment of systolic and diastolic function of both the left and right ventricles is an integral part of the assessment and management of children with heart disease. In the setting of congenital heart disease, the systemic ventricle may be a morphologic left ventricle, morphologic right ventricle, or single functional ventricular chamber of right, left or indeterminate morphology. On the other hand, the subpulmonary ventricle may be a morphologic right ventricle or a morphologic left ventricle. Transthoracic echocardiography remains to be the most useful imaging

modality for evaluating cardiac function in these patient populations given its non-invasive nature and wide availability. Conventional echocardiographic assessment of cardiac function is based on two-dimensional and M-mode assessment of wall motion abnormalities, ventricular dimensions, volumes and ejection fraction, and Doppler assessment of valvar inflow and outflow for evaluation of haemodynamic alterations secondary to ventricular systolic and diastolic dysfunction. These parameters are nonetheless limited by the need for geometric assumptions, the qualitative nature of assessment of regional myocardial wall motion and thickening, lack of reproducibility, and

Strain (ϵ)

$$\epsilon = \frac{L - L_0}{L_0} = \frac{\Delta L}{L_0}$$

Strain rate
Rate by which deformation occurs (strain per unit time)



Figure 1 Definition strain and strain rate. The strain as measured using this method is the Lagrangian strain, which is based on a single reference length (L_0) against which all subsequent deformation is measured. L_0 is the reference length at the reference time point, which is usually taken at end-diastole for the assessment of ventricular strain.

their load dependence (1,2). Indeed, these conventional indices of cardiac function can be regarded as parameters of indirect changes consequential to the shortening and lengthening of the myocardium in the cardiac cycle. On the other hand, direct interrogation of the magnitude and rate of myocardial deformation may shed important lights on the understanding, diagnosis and prognosis on cardiac dysfunction in the paediatric cardiac population. In the past decade, technological advances in echocardiographic strain imaging have enabled direct interrogation of global and regional deformation of the myocardium (3-5).

What is strain imaging?

During systole, the ventricular myocardium shortens in the longitudinal and circumferential dimensions and thickens in the radial dimension. During diastole, reciprocal changes with lengthening of the myocardium in the longitudinal and circumferential dimensions and thinning in the radial dimension occur. Strain imaging enables direct evaluation of systolic and diastolic deformation of the myocardium throughout the cardiac cycle, which is quantified by the values of strain and strain rate (6).

Strain is defined as the change in length of a segment of myocardium relative to its resting length and is expressed as a percentage. Although the three-dimensional organization of myocardial fibres results in strain vectors that occur in a three-dimensional manner, most clinical and research applications have relied on the assessment of myocardial strain in each of the principal dimensions. Accordingly linear strain is defined by the formula $\epsilon = \Delta L/L_0$, where ϵ = strain, ΔL = change in length, and L_0 = original length (*Figure 1*). During cardiac systole, the ventricular myocardium shortens in the longitudinal

and circumferential dimensions and thickens in the radial dimension. By convention, negative strain represents shortening in the longitudinal and circumferential dimensions during systole and thinning in the radial dimension during diastole, while positive strain describes longitudinal and circumferential myocardial lengthening during diastole and radial myocardial thickening during systole. The velocity of myocardial deformation in the respective dimensions is quantified by the strain rate.

Evolution of techniques in strain imaging

Myocardial strain can be assessed in the experimental setting by implantation of sonomicrometry crystals at different ventricular myocardial segments and recording the changes in myocardial length during the cardiac cycle as measured from the transit time of ultrasound between the crystals (7). Magnetic resonance imaging-based myocardial tagging has been used to assess myocardial strain in clinical patients (8), although the technique is limited by the relatively low temporal resolution, restricted availability, and expense. In the past decade, extension of strain imaging technology to two- and three-dimensional echocardiography has broadened its utilization in children with heart diseases. With regard to echocardiographic strain analysis, the technology has evolved from one-dimensional tissue Doppler imaging (9,10) to two- and, more recently, to three-dimensional speckle tracking echocardiography (11-18).

Tissue Doppler imaging quantifies regional myocardial tissue velocities and the velocity gradient along the length of the ventricular wall, based on which regional strain and strain rate can be derived (9,10) (*Figure 2*). This technique nonetheless suffers from major limitations. These include angle dependency, noisy signals with generation of strain and strain rate curves of suboptimal quality, confinement of assessment to myocardial segments along the direction of the ultrasound beam, and confounding interpretation of results due to tethering of non-contractile scar tissue and cardiac translational movements (4-6).

Two-dimensional speckle tracking echocardiography overcomes some of the limitations of tissue Doppler imaging and has emerged as a largely angle-independent echocardiographic modality for analysis of myocardial strain (11,13). Speckles are natural acoustic markers generated from the reflection, interference, and scattering of ultrasound beams in myocardial tissue. The two-dimensional speckle tracking algorithm searches for the

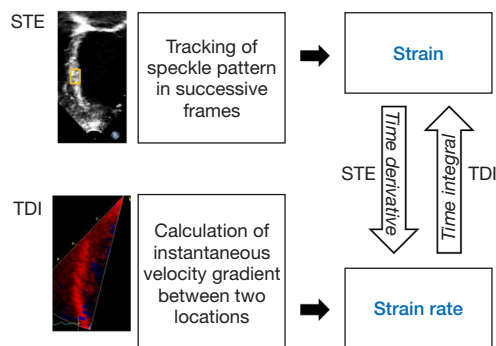


Figure 2 Principles of derivation of strain and strain rate by speckle tracking echocardiography (STE) and Doppler tissue imaging (DTI). Speckle tracking echocardiography determines myocardial strain by tracking the position of speckles in successive frames of the cardiac cycle and calculates strain rate from the derivative of strain with respect to time. On the other hand, Doppler tissue imaging determines strain rate based on the instantaneous velocity gradient between two locations in the myocardium and calculates myocardial strain by integration of strain rate over time.

location of speckles in successive frames, determines their spatial displacement, and quantifies myocardial strain in a largely angle-independent manner (*Figure 2*). Global and regional myocardial strain can be assessed in three principal dimensions of deformation: longitudinal, circumferential, and radial. The strain rate is then derived from the linear displacement of the speckles divided by the time interval between successive frames. Strain assessment using two-dimensional speckle tracking has demonstrated good correlation with sonomicrometry and myocardial tagging with magnetic resonance imaging (13,14). Additionally, this technique can be applied to images of adequate quality post hoc in a vendor-independent platform. There are, however, shortcomings inherent to two-dimensional nature of this technique. These include the failure to track out-of-plane motion of the speckles, inaccurate use of foreshortened views to assess longitudinal strain, and the need to perform basal and apical acquisitions separately for assessment of torsional mechanics.

To address these limitations and to provide comprehensive evaluation of three-dimensional ventricular mechanics, novel three-dimensional speckle tracking technology has been developed (15,16). The three-dimensional speckle tracking algorithm tracks the volumetric box templates, based on generation of cubes with the centre being the motion estimation point for tracking in successive volumes of the

cardiac cycle, in the echocardiographic three-dimensional dataset (7,16). Compared with two-dimensional speckle tracking, three-dimensional speckle tracking is limited to a lower frame rate and requires more complex processing. Nevertheless, this novel imaging modality has also been applied in the paediatric population (17,18) and confers the potential advantages of being able to track speckles beyond the two-dimensional plane, minimizing errors caused by heart-rate variability with separate acquisitions, and efficient utilization of single acquisition with simultaneous assessment of global and regional myocardial mechanics.

Assessment of ventricular and atrial strain

LV strain

Studies on LV myocyte arrangements have revealed continuum of helical fibre geometries, with the subendocardial region having a right-handed helical myofibre geometry, which changes gradually into a left-handed helical geometry in the subepicardium (19-21). Hence, the myocardial fibres are oriented longitudinally in the subendocardium, circumferentially in the mid wall, and obliquely in the subepicardium. During systole, the left ventricular myocardial fibres shorten in the longitudinal and circumferential dimensions. The longitudinal and circumferential systolic strain shows a small apex-to-base gradient, with strain values being higher in apical and mid segments compared with the basal segments (5). Shortening and shearing of myocardial fibres in the longitudinal and circumferential directions result in systolic thickening of the myocardium in the radial dimension based on the conservation of mass.

In studies of LV strain in children, the six-segment method of LV strain quantification is commonly used. Ventricular end-diastole based on the onset of QRS complex is used as the reference time point when quantifying ventricular strain. Longitudinal strain is obtained from the average of the six segments from the apical four-chamber view, and circumferential strain and radial strain from averages of the six segments from the mid-ventricular level at the papillary muscle (*Figure 3*). On the other hand, LV global longitudinal strain (GLS) and strain rate can also be calculated from a 17- or 18-segment model from segmental averaging of the apical four-, three-, and two-chamber views, while global circumferential strain (GCS) and global radial strain (GRS) can be calculated from segmental averaging of the short-axis views at the apical, mid-ventricular, and basal levels.

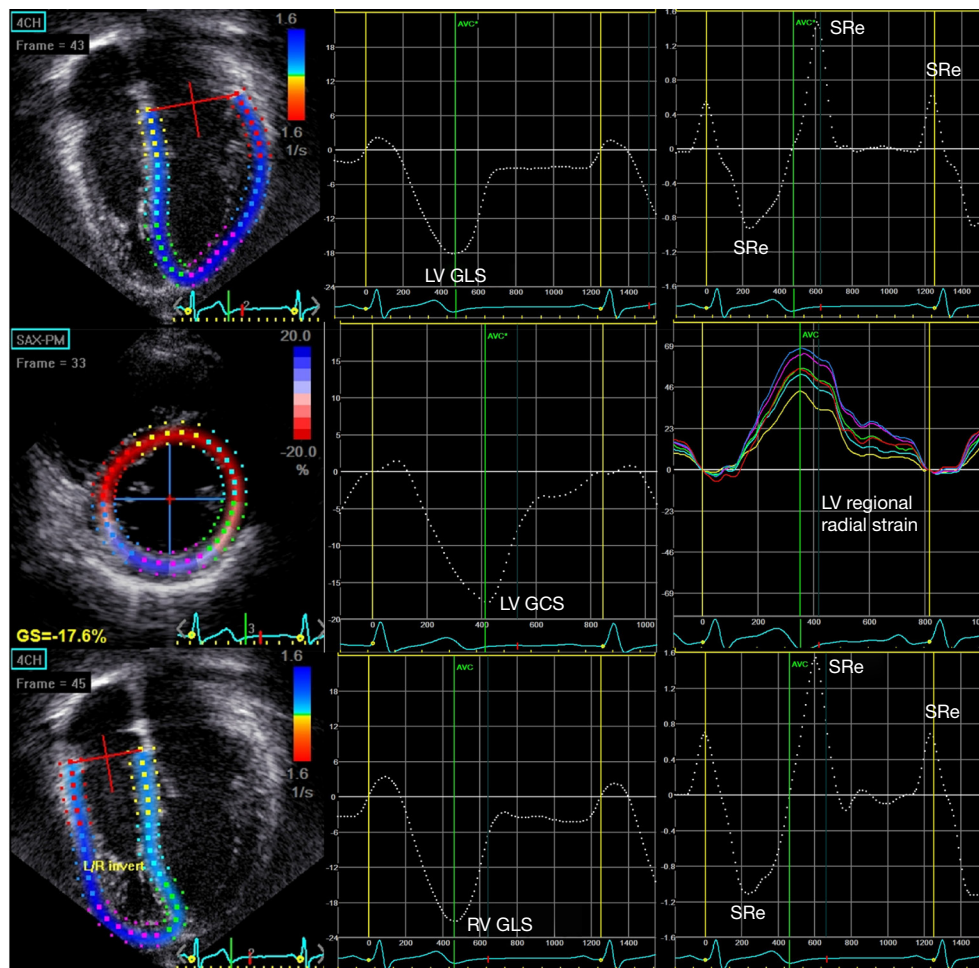


Figure 3 Illustrations of two-dimensional speckle tracking for quantification of left ventricular (LV) global longitudinal (GLS) and systolic (SRs) and early (SRe) and late (SRa) diastolic strain rates (upper panels), LV global circumferential strain (GCS) and regional radial strain (middle panels) and right ventricular (RV) GLS, SRs, SRe, and SRa (lower panels).

RV strain

Longitudinal shortening of the myocardial fibres of the RV free wall and ventricular septum is the major contributor of RV performance. By contrast to the relatively more homogenous distribution of strain within the left ventricle, the strain distribution is less homogeneous in the right ventricle. There is an obvious apex-to-base gradient, with strain values highest in the apical segments and outflow tract (5). Right ventricular longitudinal function can be assessed by quantification of RV GLS based on the entire traced contour of the right ventricle including the free wall and septum from the apical four-chamber (*Figure 3*) or RV free wall strain obtained from the average strain of the basal, middle, and apical segments of the RV lateral free wall.

Atrial strain

The atrium transforms continuous venous return into intermittent ventricular filling and serves the function of a reservoir, a conduit, and a pump (22). As a reservoir, the atrium collects blood from either the systemic or pulmonary venous return and fills during ventricular systole. As a conduit, the atrium allows the passage of the blood to either the right or the left ventricle during early ventricular diastole. As a pump, the atrium contracts during late ventricular diastole. Assessment of atrial strain and strain rate in different phases of the cardiac cycles may permit the evaluation of individual components of atrial function (*Figures 4, 5*).

Nomenclature for atrial strain imaging depends on the

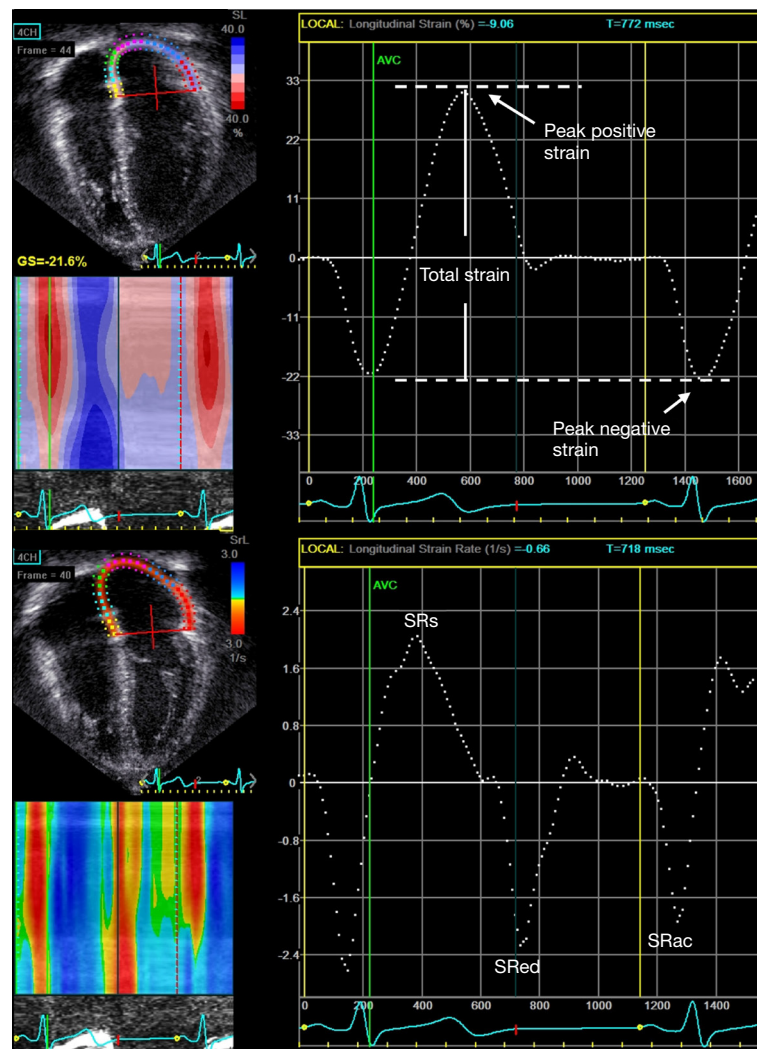


Figure 4 Utilization of two-dimensional speckle tracking for quantification of left atrial strain and strain rates at ventricular systole (SRs) and early diastole (SRe) and at atrial contraction (SRac). The onset of P wave is taken as the reference time point.

selection of the reference time point, which can either be the onset of the P (atrial contraction) or QRS (ventricular end-diastole) wave. Using P wave onset as the reference time point, the negative strain corresponds to atrial contraction, the positive strain corresponds to conduit function, and the total strain corresponds to reservoir function (Figures 4,5). When QRS wave is used as the reference time point, the peak atrial strain represents the reservoir function, while the peak atrial contraction strain represents the pump function. The strain rate at atrial contraction, ventricular systole, and ventricular diastole reflects pump, reservoir, and conduit function, respectively.

Reference values of myocardial strain in children

Systematic reviews and meta-analyses have been performed to determine the normal range of the left and right ventricular strain measurements in children (23,24).

To establish the reference paediatric range of LV strain and strain rate as measured by two-dimensional speckle tracking, Levy *et al.* performed a systematic review and identified 2,325 children from 43 data sets (23). They stratified their meta-analysis results based on the methods (global strain versus six-segment method) of LV strain analysis. Global LV longitudinal strain (GLS) and strain

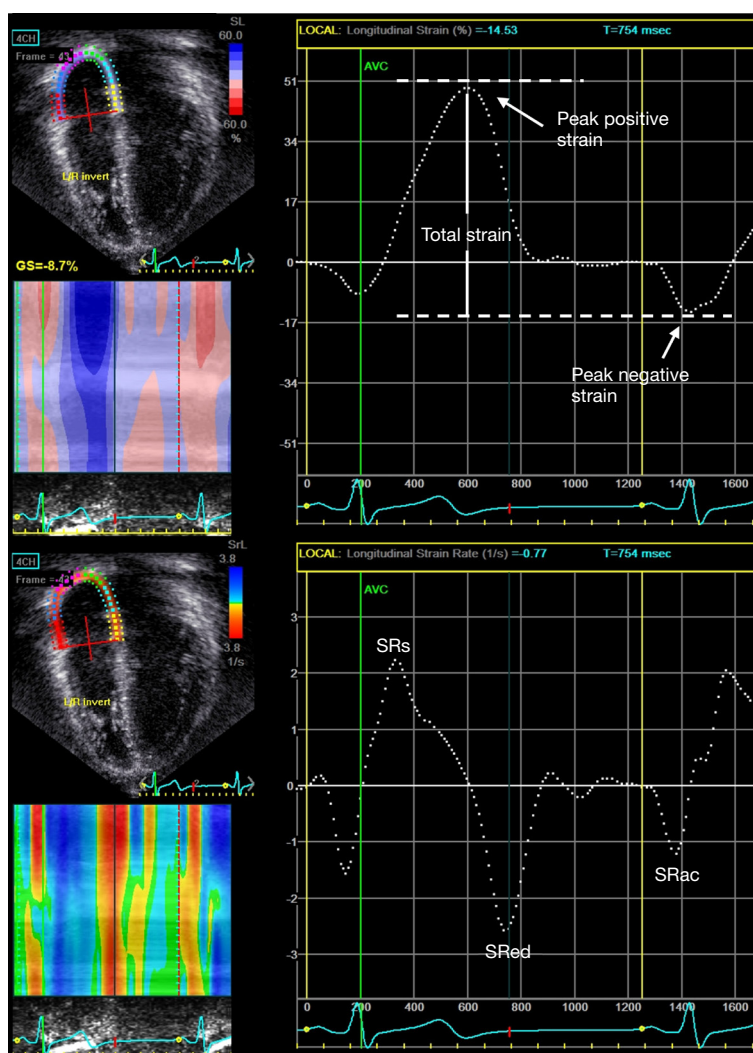


Figure 5 Utilization of two-dimensional speckle tracking for quantification of right atrial strain and strain rates at ventricular systole (SRs) and early (SRe) and at atrial contraction (SRac). The onset of P wave is taken as the reference time point.

rate was calculated from a 17- or 18-segment model from segmental averaging of the three apical views (apical four, three-, and two-chamber), while GCS and GRS were calculated from segmental averaging of the short-axis views at the apical, mid-ventricular, and basal levels. The six-segment method was commonly used in studies of LV mechanics in children. Longitudinal strain was obtained from the weighted average of the six segments from the apical four-chamber view, and circumferential strain and radial strain from weighted averages of the six segments from the mid-ventricular level at the papillary muscle. In healthy children the mean LV GLS was 20.2% (95% CI, -19.5% to -20.8%), mean GCS was -22.3% (95%

CI, -19.9% to -24.6%), and mean GRS was 45.2% (95% CI, 38.3% to 51.7%). Importantly, variations among different reference ranges do not appear to be dependent on differences in demographic, clinical, or equipment or vendor parameters in this meta-analysis. Normal ranges of LV three-dimensional global systolic strain in children have also been reported, although data remain limited in this regard (17).

The reference range of RV strain and strain rate as measured by two-dimensional speckle-tracking echocardiography was also reported by the same group of investigators who performed a systematic review and meta-analysis of 226 children from 10 studies (24). They stratified

their meta-analysis results based on the methods (global longitudinal strain versus free wall strain) of RV strain analysis. Right ventricular GLS was calculated based on the entire traced contour of the right ventricle including the free wall and septum from the apical four-chamber view, while RV free wall strain was obtained from the weighted average of the basal, mid, and apical segments of the RV lateral free wall. The normal mean value in children for RV GLS was -29.03% (95% CI, -31.52% to -26.54%). Similar to those of LV strain, variations in RV strain among different normal ranges did not appear to be dependent on differences in demographic, clinical, or equipment parameters.

The normal reference ranges of LA and RA reservoir and contractile strain as assessed by two-dimensional speckle tracking echocardiography have also been reported in infants and children (25). Importantly, this study showed little variation of atrial strain parameters with age.

Echocardiographic strain imaging in children with congenital heart disease

Strain imaging has increasingly been utilized to assess RV and LV performance in children, adolescents and adults with various types of congenital and acquired heart diseases. The relatively angle-independent two-dimensional speckle tracking echocardiography has emerged as the technology of choice for assessment myocardial strain in various congenital heart conditions as discussed below.

Tetralogy of Fallot (TOF)

In patients with TOF, dysfunction of the right and left ventricles is an important issue even long term after repair. Adverse remodeling of the right ventricle related to chronic pulmonary regurgitation, use of transannular patch, electromechanical dyssynchrony, and myocardial fibrosis may impair RV function. Ventricular-ventricular interaction may further predispose to development of LV dysfunction in these patients. Data on the use of myocardial strain imaging in assessing cardiac mechanics and its clinical and prognostic values are accumulating in these patients.

We have recently reviewed the use of strain imaging in assessing RV and LV mechanics, associations between RV and LV deformation, changes in ventricular deformation after pulmonary valve replacement, and associations between measures of RV and LV deformation and outcomes in patients with repaired TOF (26). Most of the strain imaging studies have shown reduction of RV global and

regional systolic strain and strain rate in repaired TOF patients (27-32). Impairment of RV deformation has been shown to associate with reduced RV ejection fraction (33), ventricular dyssynchrony (34,35), and greater severity of pulmonary regurgitation (36,37). With regard to LV strain analysis in these patients, we (36) and others (27,37-39) have reported on significant reduction of LV systolic longitudinal, circumferential, and radial strain. Correlations between LV and RV strain parameters provide evidence of ventricular-ventricular interaction in these patients. Studies on the impact of pulmonary valve replacement of RV and LV strain have yielded, however, inconsistent results (40-42). However, the prognostic value of LV and RV strain in adults with repaired TOF was shown in studies that found associations between LV global longitudinal strain (43,44) and RV free wall longitudinal strain (44) and adverse cardiovascular outcomes including sudden cardiac death, heart failure and/or life-threatening ventricular arrhythmia.

We further performed a systematic review of 10 studies of atrial strain imaging, which involved 536 adolescent and adult patients with repaired TOF (45). Of the 10 studies, seven used speckle tracking echocardiography, two used tissue Doppler imaging and one used cardiac magnetic resonance feature tracking. The main findings were reduced regional and/or global RA and LA strain and strain rate consistent with reduced conduit, reservoir and contractile function of the two atria in patients, associations between RA and LA deformation indices suggestive of atrial-atrial interaction, and relationships between RA deformation and indices of right ventricular systolic and diastolic function. However, the lack of data on prognostic value of atrial strain was identified as an important knowledge gap.

Pulmonary atresia with intact ventricular septum (PAIVS) and pulmonary stenosis

In PAIVS and severe pulmonary stenosis, the hypertrophic myocardium and varying degrees of endocardial fibroelastosis may provide anatomic substrates for restrictive RV physiology. In patients after biventricular repair of PAIVS, we have shown using two-dimensional speckle tracking impairment of RV systolic and diastolic strain (46). Patients with a restrictive RV physiology, compared to those without, had lower RV global systolic strain and lower RV systolic and early diastolic strain rates. These findings suggest that RV diastolic strain assessment may be useful in the assessment of RV diastolic function. We further reported recently impairment of RA strain in patients' long term after repair of

PAIVS and pulmonary stenosis and its associations with RV diastolic dysfunction, longer P-wave duration, greater P-wave dispersion (47), and increased liver stiffness (48).

Transposition of the great arteries post atrial switch operation

Dysfunction of the systemic right ventricle is an important concern in patients after Senning or Mustard operation for complete transposition of the great arteries (TGA) (49,50). Anatomic, haemodynamic and surgical factors and the fibrotic myocardium may contribute to systemic RV dysfunction in these patients. We (51) and others (52-56) have demonstrated usefulness of strain imaging in the assessment of systemic RV function. Systemic RV longitudinal strain and strain rate were found to correlate with cardiac magnetic resonance-derived systemic RV ejection fraction (51). Furthermore, Ladouceur *et al.* found that only systemic RV GLS but not ejection fraction showed significant correlation with functional capacity as measured by peak oxygen uptake during exercise testing (56). Using cardiac magnetic resonance, Pettersen *et al.* unveiled predominant circumferential over longitudinal free wall shortening in the systemic right ventricle, which resembles that found in the normal left ventricle, but opposite to the findings in a normal subpulmonary right ventricle (52). The shift from longitudinal shortening to transverse thickening as assessed by radial strain assessment of the systemic right ventricle has also been found to correlate with exercise capacity in patients after atrial switch operation (55). Strain imaging can also help to define the magnitude of intra-systemic RV and inter-ventricular mechanical delay in these patients (57), which may exert negative influence on systemic RV ejection fraction and exercise capacity. Additionally, strain imaging studies have revealed unfavourable systolic (58) and diastolic (59) interaction between the subpulmonary left ventricle and the systemic right ventricle. The prognostic value of systemic RV global longitudinal strain was shown by studies showing its ability to predict adverse clinical outcomes including symptomatic progression to worse functional class, development of cardiac arrhythmias, and death in patients after atrial switch operation (58,60).

Congenitally corrected transposition of the great arteries

In congenitally corrected TGA, the systemic RV peak systolic strain and strain rate have been shown to be

reduced (61). Pulmonary artery banding, as a management option for patients with failing systemic right ventricles, may reduce septal shift to reduce tricuspid regurgitation and improve systemic RV geometry (62). However, this may cause acute reduction in global subpulmonary LV strain and ejection fraction. In patients undergoing anatomic repair after LV retraining, reduction of systemic LV strain has been demonstrated (63), indicating the need for long-term monitoring of cardiac function in these patients.

Coarctation of the aorta

Systemic arterial abnormalities related to structural alteration of aortic structure and stiffening of the central arteries in patients persist despite successful interventions for coarctation of the aorta (64,65). Increased afterload may adversely impact on ventricular-arterial interaction. Previous studies have shown reduced systolic longitudinal and radial strain but with preservation of circumferential strain in these patients (66-68). Obese patients compared with non-obese ones were further found to have greater impairment of left ventricular myocardial deformation in the longitudinal, radial, and circumferential dimensions (69). Recently, we have reported on LA dysfunction in patients after repair of aortic coarctation and interruption, as evidenced by reduced LA positive and negative strain and strain rates at all phases of the cardiac cycle (70). Impairment of LA strain was found to associate with altered LV strain and increased arterial stiffness, implicating the possibility of abnormal arterial-LV-LA coupling in patients despite satisfactory repair of aortic coarctation and interruption. The prognostic implications of these findings remain, however, to be determined.

Functional single ventricle

Systolic and diastolic ventricular dysfunction in patients with a functional single ventricle post Fontan-type procedures is well documented (71,72). Impairment of myocardial strain has been shown in patients with functional single ventricles of either the right or left ventricular morphology (73-76). In patients with tricuspid atresia after Fontan procedure, we have demonstrated reduction of global systemic LV longitudinal, circumferential, and radial strain and systolic and diastolic strain rates (77). Additionally, in this study, based on three-dimensional segmental volume assessment of the systemic left ventricle, we found evidence of mechanical dyssynchrony in about half of our Fontan patients with tricuspid atresia. In children with hypoplastic

left heart syndrome, Friedberg *et al.* similarly demonstrated mechanical dyssynchrony of the systemic right ventricle using velocity vector imaging based on the principle of 2D speckle tracking (78).

Changes in systemic ventricular mechanics have been found may occur during the stages of the univentricular repair, primarily reported in patients with hypoplastic left heart syndrome. In these patients, before cavopulmonary connection, the ratio of systemic RV longitudinal to circumferential strain was decreased and became similar to systemic LV-like contraction pattern. The adaptation was associated with decreased mechanical dyssynchrony and RV end-diastolic volume (79). These adaptive mechanisms, similar to that of the systemic right ventricle in patients with complete TGA after atrial switch operation (52), may be important for long-term function of the systemic right ventricle. In patients with a functional single ventricle undergoing total cavopulmonary connection, Park *et al.* reported that preoperative circumferential strain rate was independently associated with length of hospital stay and suggested that strain assessment may improve preoperative risk stratification (80).

Left-to-right shunts

Differences in atrial strain between children undergoing surgery and those after transcatheter closure of atrial septal defect has been reported (81). The peak right and left atrial strain and strain rate were found to be significantly reduced in the surgical group as compared with the catheter interventional group and healthy children. Among patients with various types of ventricular septal defects, our group has reported on worse LV systolic deformation in patients after surgical repair of subarterial defects compared with those after patch closure of perimembranous defects (82).

Clinical translation of strain imaging

While there is obvious potential of adoption of strain imaging into the clinical care of paediatric cardiac patients, several gaps and challenges need to be addressed and overcome before its incorporation into routine clinical assessment algorithm is feasible. First, there needs to be standardization of the strain parameters to be used for serial assessment of function of the systemic left ventricle, systemic or subpulmonary right ventricle, and functional single ventricle. Based on the published data, longitudinal

strain as assessed from the apical four-chamber view appears to be a promising and an easily derived parameter for clinical use. Second, the use of strain imaging has not been formally incorporated in the paediatric cardiac clinical guidelines and patient management algorithms. The incremental value of incorporating myocardial strain imaging into the management algorithm would require further exploration. As alluded to earlier, recent studies suggested potential usefulness of strain imaging in the prognostication of the outcomes of patients with repaired TOF (43,44) and those after atrial switch operation for complete TGA (58,60). Third, the approach to intervendor differences in the quantification of myocardial strain remains to be defined. The European Association of Cardiovascular Imaging and the American Society Echocardiography have convened a task force to assess variability in speckle-tracking echocardiographic measurements, aiming to standardize speckle tracking-based strain imaging as a clinical tool for assessment of cardiac function (83). The findings show that LV GLS has reproducibility superior to conventional echocardiographic measures, small but significant differences between vendors, and that GLS may be used in clinical practice (84). On the hand, the task force reported that LV segmental longitudinal strain measurements have a higher variability on top of the known intervendor bias and recommended that single segmental strain values should be used with caution and that regional strain pattern analysis may be a more robust alternative (85). Finally, strain parameters remain relatively load dependent (6) and need to be interpreted with caution when significant changes in preload and/or afterload occur in the longitudinal follow-up of different congenital heart populations.

Conclusions and future directions

Echocardiographic strain imaging has been used as a research tool in the interrogation of early subclinical impairment of the systemic left ventricle, systemic or subpulmonary right ventricle and functional single ventricle in different congenital heart populations. The strain parameters have been associated with other indices of ventricular function, exercise parameters, and clinical outcomes. Importantly, emerging data suggest potential prognostic values of strain measures in the prediction of occurrence of adverse cardiovascular outcomes in these at-risk populations. It is timely for paediatric cardiologists to consider the incorporation of strain imaging into the clinical management algorithm.

Acknowledgments

Funding: None.

Footnote

Provenance and Peer Review: This article was commissioned by the editorial office, *Pediatric Medicine* for the series “Advances in Pediatric Cardiology”. The article has undergone external peer review.

Conflicts of Interest: The author has completed the ICMJE uniform disclosure form (available at <https://pm.amegroups.com/article/view/10.21037/pm-21-39/coif>). The series “Advances in Pediatric Cardiology” was commissioned by the editorial office without any funding or sponsorship. YFC serves as an unpaid editorial board member of *Pediatric Medicine* from October 2020 to September 2022 and served as the unpaid Guest Editor of the series. The author has no other conflicts of interest to declare.

Ethical Statement: The author is accountable for all aspects of the work in ensuring that questions related to the accuracy or integrity of any part of the work are appropriately investigated and resolved.

Open Access Statement: This is an Open Access article distributed in accordance with the Creative Commons Attribution-NonCommercial-NoDerivs 4.0 International License (CC BY-NC-ND 4.0), which permits the non-commercial replication and distribution of the article with the strict proviso that no changes or edits are made and the original work is properly cited (including links to both the formal publication through the relevant DOI and the license). See: <https://creativecommons.org/licenses/by-nc-nd/4.0/>.

References

- Gottdiener JS, Bednarz J, Devereux R, et al. American Society of Echocardiography recommendations for use of echocardiography in clinical trials. *J Am Soc Echocardiogr* 2004;17:1086-119.
- Lang RM, Bierig M, Devereux RB, et al. Recommendations for chamber quantification: a report from the American Society of Echocardiography's Guidelines and Standards Committee and the Chamber Quantification Writing Group, developed in conjunction with the European Association of Echocardiography, a branch of the European Society of Cardiology. *J Am Soc Echocardiogr* 2005;18:1440-63.
- Shah AM, Solomon SD. Myocardial deformation imaging: current status and future directions. *Circulation* 2012;125:e244-8.
- Gorcsan J 3rd, Tanaka H. Echocardiographic assessment of myocardial strain. *J Am Coll Cardiol* 2011;58:1401-13.
- Mor-Avi V, Lang RM, Badano LP, et al. Current and evolving echocardiographic techniques for the quantitative evaluation of cardiac mechanics: ASE/EAE consensus statement on methodology and indications endorsed by the Japanese Society of Echocardiography. *Eur J Echocardiogr* 2011;12:167-205.
- Amzulescu MS, De Craene M, Langet H, et al. Myocardial strain imaging: review of general principles, validation, and sources of discrepancies. *Eur Heart J Cardiovasc Imaging* 2019;20:605-19.
- Seo Y, Ishizu T, Enomoto Y, et al. Validation of 3-dimensional speckle tracking imaging to quantify regional myocardial deformation. *Circ Cardiovasc Imaging* 2009;2:451-9.
- Petitjean C, Rougon N, Cluzel P. Assessment of myocardial function: a review of quantification methods and results using tagged MRI. *J Cardiovasc Magn Reson* 2005;7:501-16.
- Heimdal A, Støylen A, Torp H, et al. Real-time strain rate imaging of the left ventricle by ultrasound. *J Am Soc Echocardiogr* 1998;11:1013-9.
- Urheim S, Edvardsen T, Torp H, et al. Myocardial strain by Doppler echocardiography. Validation of a new method to quantify regional myocardial function. *Circulation* 2000;102:1158-64.
- Leitman M, Lysyansky P, Sidenko S, et al. Two-dimensional strain—a novel software for real-time quantitative echocardiographic assessment of myocardial function. *J Am Soc Echocardiogr* 2004;17:1021-9.
- Reisner SA, Lysyansky P, Agmon Y, et al. Global longitudinal strain: a novel index of left ventricular systolic function. *J Am Soc Echocardiogr* 2004;17:630-3.
- Amundsen BH, Helle-Valle T, Edvardsen T, et al. Noninvasive myocardial strain measurement by speckle tracking echocardiography: validation against sonomicrometry and tagged magnetic resonance imaging. *J Am Coll Cardiol* 2006;47:789-93.
- Pirat B, Khoury DS, Hartley CJ, et al. A novel feature-tracking echocardiographic method for the quantitation of regional myocardial function: validation in an animal model of ischemia-reperfusion. *J Am Coll Cardiol*

- 2008;51:651-9.
15. Crosby J, Amundsen BH, Hergum T, et al. 3-D speckle tracking for assessment of regional left ventricular function. *Ultrasound Med Biol* 2009;35:458-71.
 16. Takeguchi T, Nishiura M, Abe Y, et al. Practical considerations for a method of rapid cardiac function analysis based on three-dimensional speckle tracking in a three-dimensional diagnostic ultrasound system. *J Med Ultrason* (2001) 2010;37:41-9.
 17. Zhang L, Gao J, Xie M, et al. Left ventricular three-dimensional global systolic strain by real-time three-dimensional speckle-tracking in children: feasibility, reproducibility, maturational changes, and normal ranges. *J Am Soc Echocardiogr* 2013;26:853-9.
 18. Li SN, Yu W, Lai CT, et al. Left ventricular mechanics in repaired tetralogy of Fallot with and without pulmonary valve replacement: analysis by three-dimensional speckle tracking echocardiography. *PLoS One* 2013;8:e78826.
 19. Ashikaga H, van der Spoel TI, Coppola BA, et al. Transmural myocardial mechanics during isovolumic contraction. *JACC Cardiovasc Imaging* 2009;2:202-11.
 20. Covell JW. Tissue structure and ventricular wall mechanics. *Circulation* 2008;118:699-701.
 21. Sengupta PP, Korinek J, Belohlavek M, et al. Left ventricular structure and function: basic science for cardiac imaging. *J Am Coll Cardiol* 2006;48:1988-2001.
 22. Blume GG, Mcleod CJ, Barnes ME, et al. Left atrial function: physiology, assessment, and clinical implications. *Eur J Echocardiogr* 2011;12:421-30.
 23. Levy PT, Machefsky A, Sanchez AA, et al. Reference Ranges of Left Ventricular Strain Measures by Two-Dimensional Speckle-Tracking Echocardiography in Children: A Systematic Review and Meta-Analysis. *J Am Soc Echocardiogr* 2016;29:209-225.e6.
 24. Levy PT, Sanchez Mejia AA, Machefsky A, et al. Normal ranges of right ventricular systolic and diastolic strain measures in children: a systematic review and meta-analysis. *J Am Soc Echocardiogr* 2014;27:549-60, e3.
 25. Kutty S, Padiyath A, Li L, et al. Functional maturation of left and right atrial systolic and diastolic performance in infants, children, and adolescents. *J Am Soc Echocardiogr* 2013;26:398-409.e2.
 26. Li VW, Yu CK, So EK, et al. Ventricular Myocardial Deformation Imaging of Patients with Repaired Tetralogy of Fallot. *J Am Soc Echocardiogr* 2020;33:788-801.
 27. Menting ME, van den Bosch AE, McGhie JS, et al. Assessment of ventricular function in adults with repaired Tetralogy of Fallot using myocardial deformation imaging. *Eur Heart J Cardiovasc Imaging* 2015;16:1347-57.
 28. Scherptong RW, Mollema SA, Blom NA, et al. Right ventricular peak systolic longitudinal strain is a sensitive marker for right ventricular deterioration in adult patients with tetralogy of Fallot. *Int J Cardiovasc Imaging* 2009;25:669-76.
 29. Friedberg MK, Fernandes FP, Roche SL, et al. Impaired right and left ventricular diastolic myocardial mechanics and filling in asymptomatic children and adolescents after repair of tetralogy of Fallot. *Eur Heart J Cardiovasc Imaging* 2012;13:905-13.
 30. Dragulescu A, Friedberg MK, Grosse-Wortmann L, et al. Effect of chronic right ventricular volume overload on ventricular interaction in patients after tetralogy of Fallot repair. *J Am Soc Echocardiogr* 2014;27:896-902.
 31. Yim D, Hui W, Larios G, et al. Quantification of Right Ventricular Electromechanical Dyssynchrony in Relation to Right Ventricular Function and Clinical Outcomes in Children with Repaired Tetralogy of Fallot. *J Am Soc Echocardiogr* 2018;31:822-30.
 32. Bhatt SM, Wang Y, Elci OU, et al. Right Ventricular Contractile Reserve Is Impaired in Children and Adolescents With Repaired Tetralogy of Fallot: An Exercise Strain Imaging Study. *J Am Soc Echocardiogr* 2019;32:135-44.
 33. Toro KD, Soriano BD, Buddha S. Right ventricular global longitudinal strain in repaired tetralogy of Fallot. *Echocardiography* 2016;33:1557-62.
 34. Mueller M, Rentzsch A, Hoetzer K, et al. Assessment of interventricular and right-intraventricular dyssynchrony in patients with surgically repaired tetralogy of Fallot by two-dimensional speckle tracking. *Eur J Echocardiogr* 2010;11:786-92.
 35. Friedberg MK, Fernandes FP, Roche SL, et al. Relation of right ventricular mechanics to exercise tolerance in children after tetralogy of Fallot repair. *Am Heart J* 2013;165:551-7.
 36. Cheung EW, Liang XC, Lam WW, et al. Impact of right ventricular dilation on left ventricular myocardial deformation in patients after surgical repair of tetralogy of fallot. *Am J Cardiol* 2009;104:1264-70.
 37. Kempny A, Diller GP, Orwat S, et al. Right ventricular-left ventricular interaction in adults with Tetralogy of Fallot: a combined cardiac magnetic resonance and echocardiographic speckle tracking study. *Int J Cardiol* 2012;154:259-64.
 38. Dragulescu A, Grosse-Wortmann L, Redington A, et al. Differential effect of right ventricular dilatation on

- myocardial deformation in patients with atrial septal defects and patients after tetralogy of Fallot repair. *Int J Cardiol* 2013;168:803-10.
39. Weng KP, Hung YC, Huang SH, et al. Abnormal biventricular performance in asymptomatic adolescents late after repaired Tetralogy of Fallot: Combined two-dimensional speckle tracking and three-dimensional echocardiography study. *J Chin Med Assoc* 2018;81:170-7.
 40. Sabate Rotes A, Bonnicksen CR, Reece CL, et al. Long-term follow-up in repaired tetralogy of fallot: can deformation imaging help identify optimal timing of pulmonary valve replacement? *J Am Soc Echocardiogr* 2014;27:1305-10.
 41. Yim D, Mertens L, Morgan CT, et al. Impact of surgical pulmonary valve replacement on ventricular mechanics in children with repaired tetralogy of Fallot. *Int J Cardiovasc Imaging* 2017;33:711-20.
 42. Knirsch W, Dodge-Khatami A, Kadner A, et al. Assessment of myocardial function in pediatric patients with operated tetralogy of Fallot: preliminary results with 2D strain echocardiography. *Pediatr Cardiol* 2008;29:718-25.
 43. Diller GP, Kempny A, Liodakis E, et al. Left ventricular longitudinal function predicts life-threatening ventricular arrhythmia and death in adults with repaired tetralogy of fallot. *Circulation* 2012;125:2440-6.
 44. van Grootel RWJ, van den Bosch AE, Baggen VJM, et al. The Prognostic Value of Myocardial Deformation in Adult Patients With Corrected Tetralogy of Fallot. *J Am Soc Echocardiogr* 2019;32:866-875.e2.
 45. Cheung YF, Yu CKM, So EKF, et al. Atrial Strain Imaging after Repair of Tetralogy of Fallot: A Systematic Review. *Ultrasound Med Biol* 2019;45:1896-908.
 46. Liang XC, Lam WW, Cheung EW, et al. Restrictive right ventricular physiology and right ventricular fibrosis as assessed by cardiac magnetic resonance and exercise capacity after biventricular repair of pulmonary atresia and intact ventricular septum. *Clin Cardiol* 2010;33:104-10.
 47. To AH, Lai CT, Wong SJ, et al. Right Atrial Mechanics Long-Term after Biventricular Repair of Pulmonary Atresia or Stenosis with Intact Ventricular Septum. *Echocardiography* 2016;33:586-95.
 48. Li VW, So EK, Li W, et al. Interplay between right atrial function and liver stiffness in adults with repaired right ventricular outflow obstructive lesions. *Eur Heart J Cardiovasc Imaging* 2021;22:1285-94.
 49. Lubiszewska B, Gosiewska E, Hoffman P, et al. Myocardial perfusion and function of the systemic right ventricle in patients after atrial switch procedure for complete transposition: long-term follow-up. *J Am Coll Cardiol* 2000;36:1365-70.
 50. Roos-Hesselink JW, Meijboom FJ, Spitaels SE, et al. Decline in ventricular function and clinical condition after Mustard repair for transposition of the great arteries (a prospective study of 22-29 years). *Eur Heart J* 2004;25:1264-70.
 51. Chow PC, Liang XC, Cheung EW, et al. New two-dimensional global longitudinal strain and strain rate imaging for assessment of systemic right ventricular function. *Heart* 2008;94:855-9.
 52. Pettersen E, Helle-Valle T, Edvardsen T, et al. Contraction pattern of the systemic right ventricle shift from longitudinal to circumferential shortening and absent global ventricular torsion. *J Am Coll Cardiol* 2007;49:2450-6.
 53. Eindhoven JA, Menting ME, van den Bosch AE, et al. Quantitative assessment of systolic right ventricular function using myocardial deformation in patients with a systemic right ventricle. *Eur Heart J Cardiovasc Imaging* 2015;16:380-8.
 54. Woudstra OI, van Dissel AC, van der Bom T, et al. Myocardial Deformation in the Systemic Right Ventricle: Strain Imaging Improves Prediction of the Failing Heart. *Can J Cardiol* 2020;36:1525-33.
 55. Di Salvo G, Pacileo G, Rea A, et al. Transverse strain predicts exercise capacity in systemic right ventricle patients. *Int J Cardiol* 2010;145:193-6.
 56. Ladouceur M, Redheuil A, Soulat G, et al. Longitudinal strain of systemic right ventricle correlates with exercise capacity in adult with transposition of the great arteries after atrial switch. *Int J Cardiol* 2016;217:28-34.
 57. Chow PC, Liang XC, Lam WW, et al. Mechanical right ventricular dyssynchrony in patients after atrial switch operation for transposition of the great arteries. *Am J Cardiol* 2008;101:874-81.
 58. Diller GP, Radojevic J, Kempny A, et al. Systemic right ventricular longitudinal strain is reduced in adults with transposition of the great arteries, relates to subpulmonary ventricular function, and predicts adverse clinical outcome. *Am Heart J* 2012;163:859-66.
 59. Chow PC, Liang XC, Cheung YF. Diastolic ventricular interaction in patients after atrial switch for transposition of the great arteries: a speckle tracking echocardiographic study. *Int J Cardiol* 2011;152:28-34.
 60. Kalogeropoulos AP, Deka A, Border W, et al. Right ventricular function with standard and speckle-tracking

- echocardiography and clinical events in adults with D-transposition of the great arteries post atrial switch. *J Am Soc Echocardiogr* 2012;25:304-12.
61. Bos JM, Hagler DJ, Silvairat S, et al. Right ventricular function in asymptomatic individuals with a systemic right ventricle. *J Am Soc Echocardiogr* 2006;19:1033-7.
 62. Filippov AA, Del Nido PJ, Vasilyev NV. Management of Systemic Right Ventricular Failure in Patients With Congenitally Corrected Transposition of the Great Arteries. *Circulation* 2016;134:1293-302.
 63. Sun HY, Behzadian F, Pun R, et al. Decremental left ventricular deformation after pulmonary artery band training and subsequent repair in ventriculoarterial discordance. *J Am Soc Echocardiogr* 2013;26:765-74.
 64. Sehested J, Baandrup U, Mikkelsen E. Different reactivity and structure of the prestenotic and poststenotic aorta in human coarctation. Implications for baroreceptor function. *Circulation* 1982;65:1060-5.
 65. de Divitiis M, Pilla C, Kattenhorn M, et al. Vascular dysfunction after repair of coarctation of the aorta: impact of early surgery. *Circulation* 2001;104:1165-70.
 66. Young AA, Cowan BR, Occlshaw CJ, et al. Temporal evolution of left ventricular strain late after repair of coarctation of the aorta using 3D MR tissue tagging. *J Cardiovasc Magn Reson* 2002;4:233-43.
 67. di Salvo G, Pacileo G, Limongelli G, et al. Abnormal regional myocardial deformation properties and increased aortic stiffness in normotensive patients with aortic coarctation despite successful correction: an ABPM, standard echocardiography and strain rate imaging study. *Clin Sci (Lond)* 2007;113:259-66.
 68. Kowalski M, Kowalik E, Kotliński K, et al. Regional left ventricular myocardial shortening in normotensive patients late after aortic coarctation repair - normal or impaired? *Ultrasound Med Biol* 2009;35:1947-52.
 69. Di Salvo G, Gala S, Castaldi B, et al. Impact of obesity on left ventricular geometry and function in pediatric patients after successful aortic coarctation repair. *Echocardiography* 2011;28:907-12.
 70. Li VW, Cheung YF. Arterial-left ventricular-left atrial coupling late after repair of aortic coarctation and interruption. *Eur Heart J Cardiovasc Imaging* 2015;16:771-80.
 71. Rychik J, Atz AM, Celermajer DS, et al. Evaluation and Management of the Child and Adult With Fontan Circulation: A Scientific Statement From the American Heart Association. *Circulation* 2019. [Epub ahead of print]. doi: 10.1161/CIR.0000000000000696.
 72. Budts W, Ravekes WJ, Danford DA, et al. Diastolic Heart Failure in Patients With the Fontan Circulation: A Review. *JAMA Cardiol* 2020;5:590-7.
 73. Singh GK, Cupps B, Pasque M, et al. Accuracy and reproducibility of strain by speckle tracking in pediatric subjects with normal heart and single ventricular physiology: a two-dimensional speckle-tracking echocardiography and magnetic resonance imaging correlative study. *J Am Soc Echocardiogr* 2010;23:1143-52.
 74. Koopman LP, Geerdink LM, Bossers SSM, et al. Longitudinal Myocardial Deformation Does Not Predict Single Ventricle Ejection Fraction Assessed by Cardiac Magnetic Resonance Imaging in Children with a Total Cavopulmonary Connection. *Pediatr Cardiol* 2018;39:283-93.
 75. Moiduddin N, Texter KM, Zaidi AN, et al. Two-dimensional speckle strain and dyssynchrony in single left ventricles vs. normal left ventricles. *Congenit Heart Dis* 2010;5:579-86.
 76. Moiduddin N, Texter KM, Zaidi AN, et al. Two-dimensional speckle strain and dyssynchrony in single right ventricles versus normal right ventricles. *J Am Soc Echocardiogr* 2010;23:673-9.
 77. Ho PK, Lai CT, Wong SJ, et al. Three-dimensional mechanical dyssynchrony and myocardial deformation of the left ventricle in patients with tricuspid atresia after Fontan procedure. *J Am Soc Echocardiogr* 2012;25:393-400.
 78. Friedberg MK, Silverman NH, Dubin AM, et al. Right ventricular mechanical dyssynchrony in children with hypoplastic left heart syndrome. *J Am Soc Echocardiogr* 2007;20:1073-9.
 79. Khoo NS, Smallhorn JF, Kaneko S, et al. Novel insights into RV adaptation and function in hypoplastic left heart syndrome between the first 2 stages of surgical palliation. *JACC Cardiovasc Imaging* 2011;4:128-37.
 80. Park PW, Atz AM, Taylor CL, et al. Speckle-Tracking Echocardiography Improves Pre-operative Risk Stratification Before the Total Cavopulmonary Connection. *J Am Soc Echocardiogr* 2017;30:478-84.
 81. Di Salvo G, Drago M, Pacileo G, et al. Atrial function after surgical and percutaneous closure of atrial septal defect: a strain rate imaging study. *J Am Soc Echocardiogr* 2005;18:930-3.
 82. Kwok SY, Yeung SS, Li VW, et al. Ventricular mechanics after repair of subarterial and perimembranous VSDs. *Eur J Clin Invest* 2017. doi: 10.1111/eci.12852.
 83. Voigt JU, Pedrizzetti G, Lysyansky P, et al. Definitions

- for a common standard for 2D speckle tracking echocardiography: consensus document of the EACVI/ASE/Industry Task Force to standardize deformation imaging. *J Am Soc Echocardiogr* 2015;28:183-93.
84. Farsalinos KE, Daraban AM, Ünü S, et al. Head-to-Head Comparison of Global Longitudinal Strain Measurements among Nine Different Vendors: The EACVI/ASE Inter-Vendor Comparison Study. *J Am Soc Echocardiogr* 2015;28:1171-81, e2.
85. Mirea O, Pagourelas ED, Duchenne J, et al. Variability and Reproducibility of Segmental Longitudinal Strain Measurement: A Report From the EACVI-ASE Strain Standardization Task Force. *JACC Cardiovasc Imaging* 2018;11:15-24.

doi: 10.21037/pm-21-39

Cite this article as: Cheung YF. Echocardiographic strain imaging: what do paediatric cardiologists need to know? *Pediatr Med* 2022;5:38.